On the Effective Thermal Conductivity of Frost Considering Mass Diffusion and Eddy convection

(Running Head: Effective Thermal Conductivity of Frost)

Max Kandula

ASRC Aerospace, John F. Kennedy Space Center, FL 32899, USA

E-mail address: max.kandula-1@nasa.gov

Abstract

A physical model for the effective thermal conductivity of water frost is proposed for application to the full range of frost density. The proposed model builds on the Zehner-Schlunder one-dimensional formulation for porous media appropriate for solid-to-fluid thermal conductivity ratios less than about 1000. By superposing the effects of mass diffusion and eddy convection on stagnant conduction in the fluid, the total effective thermal conductivity of frost is shown to be satisfactorily described. It is shown that the effects of vapor diffusion and eddy convection on the frost conductivity are of the same order. The results also point out that idealization of the frost structure by cylindrical inclusions offers a better representation of the effective conductivity of frost as compared to spherical inclusions. Satisfactory agreement between the theory and the measurements for the effective thermal conductivity of frost is demonstrated for a wide range of frost density and frost temperature.

Key Words: Water frost, effective thermal conductivity, Zehner-Schlunder model, porous media, vapor diffusion, eddy convection

Nomenclature

A_{fs} interface area in Zehner-Schlunder model, m^2

D mass diffusion coefficient, m^2/s

h_{sv} latent heat of sublimation, J/kg

k thermal conductivity, W/m.K

k_{ef} effective thermal conductivity of frost, W/m.K

M molecular weight, kg/mol

p pressure, Pa

p_v partial pressure of water vapor at temperature T, Pa

p_{v0} partial pressure of water vapor at temperature T_0, Pa

Pr Prandtl number

$\overline{R}$ universal gas constant, J/mol.K

R_a gas constant for air, J/kg.K

R_v gas constant for water vapor, J/kg.K

r radial coordinate, m

T temperature, K

T_f frost temperature, K

T_∞ freestream temperature, K

U_∞ freestream velocity, m/s

z axial coordinate, m

Greek Symbols

ϕ solids fraction

ψ porosity (void fraction)

ν kinematic viscosity, m^2/s

λ solid-to-fluid thermal conductivity ratio, k_2 / k_1

ρ_f frost density, kg/m^3

ξ fluid-to-solid thermal conductivity ratio, k_1 / k_2

ω humidity ratio of moist air, kg (water vapor)/kg(dry air)

ΔT temperature difference in the enclosure for natural convection, K

Subscripts

1 continuous medium (stagnant gas)

2 solid particle (dispersed)

∞ ambient

a dry air

c eddy convection

d diffusion

e effective medium

f frost

s frost surface

t total (ambient)

v water vapor

1. Introduction

Frost formation represents an important consideration in cryogenics, refrigeration, aerospace, meteorology and various process industries. Processes involving simultaneous heat transfer and frost formation are occasioned in gas coolers, refrigerators, regenerators, freeze-out purification of gases, cryopumping, and the storage of cryogenic liquids.

In most technical applications frosting is undesirable, except in situations such as freeze-drying of foods. Frost offers significant thermal resistance to heat transport in heat exchangers, and increases the pressure drop by flow restriction. For example, under certain circumstances frost formation can result in 50 to 75% decrease in heat transfer and a substantial increase in pressure drop (Emery and Siegel, 1990). Nocturnal frost/icing on aircraft wings causes significant aerodynamic penalties in lift and drag (Sahin, 2000), leading to a decrease in lift and an increase in drag. Frost/ice formation on cold fuel/oxidizer tanks and other components may cause debris concerns when it is shed on critical components. A fundamental understanding of the nature of frost formation and simultaneous heat and mass transfer during frost growth is thus of great practical interest.

Frost forms when moist (humid) air comes in contact with a cold surface whose temperature is less than the freezing temperature of water (273 K), and is less than the dew point temperature, so that water vapor directly passes from a gaseous state to solid state (see Burghardt, 1972). The thermodynamic process of frost nucleation is represented with the aid of a psychrometric chart (Piucco et al., 2008).

Among the transport properties of frost (regarded as a porous medium), the effective thermal conductivity of frost primarily governs the heat transport through the frost layer and its growth rate. Measurements by various investigators suggest that the effective

thermal conductivity of frost depends on a number of parameters such as frost density, frost temperature, plate surface temperature, and environmental parameters (air temperature T_∞, humidity ω_∞, velocity U_∞, etc.), the frost density and frost temperature being the most important variables. As frost grows on the cold surface and densifies, both the thermal conductivity and density increase by an order of magnitude. Several empirical correlations have been proposed for the effective thermal conductivity of frost (as a function of frost density/or temperature), and form the basis for many theoretical models for predicting frost growth.

An accurate description of the effective frost conductivity is exceedingly difficult. This is evident from the nonhomogeneous character of the porous medium, comprised of ice particles of various shapes and sizes distributed in moist air, and their interaction involving heat and mass transfer. The structure of frost, regarded as a porous medium, consisting of different grain (pore) sizes and geometries, thus results in the effective thermal conductivity that is far from isotropic. Many models are therefore based on the assumption of uniform-sized particles of relatively simple geometry with periodic (regular) structures, such as simple cubic (SC), face-centered cubic (FCC) and body-centered cubic (BCC), and are generally limited to a narrow range of frost density (solids fraction). For example, the maximum values of solid fraction that is possible in a packed bed of uniform spherical particles are 0.5236, 0.68 and 0.74 for SC, BCC and FCC types of packing respectively (Tien and Vafai 1979). Tien and Vafai (1979) have shown that the SC packing and FCC packing respectively yield lower and upper bounds for the effective thermal conductivity of a random packed bed. For cylindrical particles, the SC packing yields the limit of $\phi = 0.7854$.

Woodside (1958) proposed a model for the thermal conductivity of snow by considering the medium to be composed of a cubic lattice of uniform solid spherical particles suspended in a gas, and including the effect of mass diffusion. This model considered a unit cube containing one-eighth of a sphere of radius less than or equal to unity. Woodside's equation when compared to the thermal conductivity of Pitman and Zuckerman (1967) for snow at -88 ^{0}C, -27 ^{0}C, and -5 ^{0}C suggest that it predicts considerably steep variation with density for densities in excess of about 400 to 500 kg/m^3. The model is limited to solids fraction of $\phi = 0.5236$ (touching spheres) as a result of the unit cube considered.

Dietenberger (1983) developed a semi-theoretical expression for the frost conductivity for the whole range of frost density by postulating a complicated frost structure. A random mixture model was proposed with ice cylinders and spheres immersed in moist air at low densities, and with ice planes and moist air bubbles at high densities. Mass diffusion is also included, and the frost conductivity is shown to depend on both frost density and frost temperature. The predicted frost conductivity at high densities undergoes steep variation, and considerably (rather unrealistically) exceeds the measurements.

Le Gall et al. (1987) considered the model of Auracher (1986) for modeling the conductivity of frost as a function of both temperature and density . The model is applicable for the full range of solids fraction. Apparently unreasonably large values of mass diffusion rates (relative to molecular diffusion rates) were postulated to match the model with measurements.

Sahin (2000) developed a model of the effective thermal conductivity of frost during the *initial crystal growth period*, by regarding the frost as formed of cylindrical frost

columns (normal to the cold surface) surrounded by moist air, and taking into account mass diffusion. Although the model seems to be physically realistic and consistent with observed frost structure, its application is limited to early stages of frost formation.

In most of the theoretical models, the contributions of radiation and convection to the effective thermal conductivity of frost have been ignored, and only vapor diffusion contribution is considered. While the neglect of thermal radiation and natural convection is justified, the role of turbulent eddy convection is open to question. An investigation by Biguria and Wenzel (1970) suggest that the turbulent eddy conductivity becomes important, and increases in proportion to the freestream velocity.

In recent times, fractal geometry has been widely applied to predict the thermal conductivity of porous media. Yu and Cheng (2002) considered fractal models for the effective thermal conductivity of bi-dispersed porous media. The theoretical predictions based on fractal models are shown to agree well with experimental data, and the lumped parameter models (see Hsu et al. 1994, and Cheng and Hsu, 1999) based on unit cell approach. Feng et al. (2007) applied fractal geometry for investigating the effective thermal conductivity of unsaturated porous media (3-phases including a solid, a wetting phase such as water, and a non-wetting phase such as air) on the basis of self-similarity.

It is the purpose of this article to propose a theoretical model applicable for the effective thermal conductivity of frost over the full range of frost density. The model starts from a well-established porous media model devoid of mass diffusion and thermal convection effects, and superposes the effect of vapor diffusion and turbulent eddy convection on pure conduction in the fluid. The validity of the proposed model will be

assessed by comparison with existing correlations and measurements for the frost thermal conductivity over an extended range of frost density and frost temperature.

2. Frost Structure and Mechanism of Frost Formation

An understanding of the frost structure and the mechanism of frost formation is helpful in developing models for the frost conductivity. The frost growth (formation) period can be broadly divided into three periods (Cheng and Wu, 2003): 1) a crystal growth period, 2) developing frost layer growth period, and 3) fully developed frost layer growth period (Fig. 1a). In the crystal growth period representing early stage of frost formation, one-dimensional type ice columns grow out of nucleation sites. In the frost layer growth periods, three dimensional growth of ice crystals produce a porous structure of the frost layer. The full growth period may be further classified into monotonic and cyclic growth periods (Cheng and Wu, 2003).

Very little is known about the fundamental nature of the nucleation or initial stages of frost formation phenomenon; i.e. crystal structure during early stage of frost formation. The rapid frost growth rates during the initial stages of frost formation corresponds to the crystal growth period. Crystal structure may be classified as columns, plates and dendrites (Sahin, 2000), as shown in Fig. 1b. Transitions from a plate growth to prism growth , and back to a plate structure and then to prisms again have been observed as the temperature decreases. In the crystal growth period of frost formation, the frost is well represented by cylindrical frost columns (normal to the surface) surrounded by moist air (Sahin, 2000).

As frost forms, the frost surface temperature increases above the temperature of the cold surface. When the frost surface (air-frost interface) temperature approaches the freezing temperature, repeated cycles of melting and freezing occur (Sami and Duong,

1989). This results in structural changes in the frost layer that tend to increase both the density and thermal conductivity with time without a proportional (corresponding) increase in the *frost thickness*. This phenomenon is more likely to occur in high humidity and/or high temperature environments than in low humidity and low temperature environments. In the latter case, the frost surface temperature will rise to a steady value below the melting point, such that the rate of frost deposition is balanced by the rate of sublimation from the frost. Fig. 1c displays a general representation of heat and mass transport by diffusion and convection in the frost layer. Vapor transport by diffusion is known to be the main mechanism by which the temperature dependence of the thermal conductivity is manifested (Sturm et al. 1997).

Frost structure and density exert significant effect on the effective thermal conductivity of frost, and depend on frost surface temperature and the surrounding hydrodynamic (flow) conditions (Brian et al., 1970). In the low density region when the crystals commence to branch out, the convective heat transfer by *eddies* within the air space is a significant contributor to the frost thermal conductivity (Biguria and Wenzel, 1970). For example, natural convection frosts formed at low temperatures are usually light and fluffy (densities between 10 and 50 kg/m^3). Forced convection frosts formed at relatively high temperatures (248 - 247 K) have densities ranging from 300 to 500 kg/m^3, and are characterized by relatively high conductivities (Coles, 1954).

Strictly speaking, the frost conductivity and density are not uniform across the frost thickness. In view of the resulting complexity, most of the models proposed for frost growth prediction are based on the assumption that the frost density and thermal conductivity are uniform throughout the entire frost layer (Le Gall et al., 1997).

3. Correlations for Frost Thermal Conductivity

The first measurements on thermal conductivity of snow were reported by Andrews (1886). Since then many investigators reported data on the effective thermal conductivity of frost. Unfortunately, there is considerable scatter in the conductivity data arising primarily from the differences in the microstructure of snow, with differences in grain characteristics (grain size and grain type) and inter-granular bonding (connectivity), leading to an order of magnitude range in the conductivity at a given density (Sturm et al., 1997). These measurements were presented in the form of correlations of thermal conductivity as a function of density and/or temperature.

A detailed list of various correlations proposed for the effective thermal conductivity of frost along with the density limit has been presented in Shin et al. (2003) and Yang and Lee (2004). These correlations express the conductivity in terms of frost density and frost surface temperature. Most of these correlations are limited to $\rho_f < 600\,\text{kg/m}^3$.

Van Dusen (1929) proposed the following correlation for the effective thermal conductivity of frost:

$$k_{ef} = 0.029 + 0.403\text{x}10^{-3}\rho_f + 0.2367\text{x}10^{-8}\rho_f^3 \qquad (1a)$$

where k_{ef} is in W/(m.K), and ρ_f in kg/m^3. This correlation was based on the data from six other investigators. It *does not* have a restriction on the range of frost density, but is restricted to the average frost temperature to be between 243 K and 273 K. *No data on the range of air velocities and air humidity is available to the author.* This correlation is generally known to provide a lower bound for the frost conductivity. Eq. (1a) is based on the correlation of data of six other investigators.

Yonko and Sepsy (1967) suggest the following correlation for the effective frost conductivity:

$$k_{ef} = 0.024248 + 0.731\text{x}10^{-3}\rho_f + 0.1183\text{x}10^{-5}\rho_f^2 \qquad (1b)$$

where k_{ef} is in W/(m.K), and ρ_f in kg/m^3. This equation is valid for frost density $\rho_f < 573$ kg/m^3, with no lower limit. The data cover a range of humidity ω_∞ of 0.0075-0.015 (vapor)/kg (dry air), air stream velocity U_∞ of 1.3-5.3 m/s, and ambient temperature T_∞ of 295 K.

Östin and Anderson (1991) proposed the following correlation for the frost thermal conductivity:

$$k_{ef} = -8.71x10^{-3} + 4.39x10^{-4}\rho_f + 1.05x10^{-6}\rho_f^2 \qquad (1c)$$

where k_{ef} is in W/(m.K), and ρ_f in kg/m^3. This equation is valid for frost density ρ_f in the range 50-680 kg/m^3, T_f =253-258 K, and V =3 m/s.

Other familiar correlations for the frost thermal conductivity as a function of frost density were reported by Abels (1893), Jansson (1901), Devaux (1933), Kamei et al. (1950), Kandrateva (1954), and Schropp (1935). These correlations have limited range of frost density, and are indicated in Yonko and Sepsy (1967), O'Neal and Tree (1985) and Sahin (2000). Brian et al. (1970), among others, proposed a correlation for the frost thermal conductivity as function of frost density and frost surface temperature, but is limited to ρ_f <130 kg/m^3.

The frost density appearing in the correlations for the conductivity is generally correlated with frost surface temperature T_{fs}. For example, Hayashi et al. (1977) proposed the following correlation for the frost density:

$$\rho_f = 650\exp\left[0.227\left(T_{fs} - 273.15\right)\right] \tag{2}$$

where ρ_f is in kg/m^3, and T_{fs} is in degrees Kelvin. Eq. (3) is widely considered for frost growth modeling. Eq. (3) is applicable for -25 ^{0}C<T_{fs}<0 ^{0}C, air stream velocities in the range of 2-6 m/s, and at an airstream humidity ratio of 0.0075 kg (vapor)/kg (dry air).

4. Recent Investigations on Frost Thermal Conductivity

Since the publication of Woodside (1958) model and the measurements of Pitman and Zuckerman (1967), many investigators studied the thermal conductivity of snow. Most notable among recent experimental work is that of Sturm et al. (1997), which is arguably the standard reference for snow thermal conductivity measurements. The correlation proposed by Sturm et al. (1997) is expressed by

$$\begin{aligned} k_{ef} &= 0.138 - 1.01\text{x}10^{-3}\rho_f + 3.233\text{x}10^{-6}\rho_f^2 \quad 156 \le \rho_f \le 600 \\ &= 0.023 + 0.234\text{x}10^{-3}\rho_f \qquad\qquad\qquad \rho_f \le 156 \end{aligned} \tag{3}$$

where ρ_f is in kg/m^3, and k_{ef} in W/m.K. This correlation is based on very detailed and consistent set of data (488 measurements) obtained by the transient method (short test duration) with cylindrical samples (of various types of snow) placed in an environmental chamber (to control the sample temperature).

Recently, the thermal conductivity of snow has been modeled by Kaempfer et al. (2005) as a complex porous media with the aid of three-dimensional geometries of snow structure. Kaempfer et al. (2005) also compared their model thermal conductivity with a single point

measurement at a density of 268 kg/m^3 ($\phi = 0.29$). More complex snow geometries were incorporated in the models of Aron and Colbeck (1995, 1998).

In this manner, much work has been done to improve the models of thermal conductivity through microstructure, well beyond assuming a simplified geometry of spheres.

5. Proposed Model

In the proposed theory, we regard the frost as a porous medium. We consider as a starting point the model of Zehner and Schlunder (1970) established for packed beds, which is known to be valid for the full range of void fractions and for solid-to-fluid conductivity ratio less than 1000 (Cheng and Hsu, 1999; see also Kaviany 1995). As the ice to air thermal conductivity ratio is about 100, the choice of Zehner-Schlunder model is justified for our current purposes. Vapor mass diffusion and forced convection effects are then taken into account to arrive at the effective frost thermal conductivity.

The following physical assumptions are made:

(a) Heat transfer in the frost layer is primarily one-dimensional.

(b) Frost density and thermal conductivity are independent of frost thickness.

(c) Thermal radiation within the frost layer is negligible This is so considering that the frost temperatures are low. Dietenberger (1983) has shown that for ice crystals the radiation effective conductivity is negligible for the size of ice crystals and the temperature levels of the frost layer (an order of magnitude less than the thermal conductivity of air).

(d) The gas spaces in the frost layer are small enough that heat transfer by natural convection within the frost layer is negligible. The effect of natural convection in porous frost layers is manifest on account of convective currents (Benard convection represented by a pattern of hexagonal cells) set up in enclosed spaces under certain conditions of unstable

configuration. Natural convection becomes significant only when the gas-filled spacing is of the order of 1 cm (Woodside, 1958).

(e) The total gas pressure is constant within the frost layer, and is equal to the atmospheric pressure (Le Gall et al., 1997).

(f) Soret and Dufour effects are negligible (Le Gall et al., 1997).

(g) The local humidity of air in the frost layer corresponds to saturation humidity at that temperature (thermodynamic equilibrium).

A description of the various components of the effective thermal conductivity is provided below.

5.1. Packed Bed Stagnant Thermal Conductivity

Many theoretical models for the effective thermal conductivity of porous packed beds were developed since the classical work of Maxwell (1873) and of Lord Rayleigh (1892), which were limited to relatively small solids fraction.

Zehner and Schlunder (1970) arrived at an analytical expression for the effective stagnant thermal conductivity of a packed bed . They considered for the unit cell one-eighth of a cylinder (inner cylinder of unit radius and outer cylinder of radius R), see **Fig 2**. Fluid is filled between the inner and outer cylinders while the inner cylinder consists of both the solid phase (shaded area) and the fluid phase with the interface area A_{fs} described by (Cheng and Hsu' 1999)

$$r^2 + \frac{z^2}{[B-(B-1)z]^2} = 1 \qquad (4a)$$

where r and z refer to the cylindrical coordinates (Fig. 2), and B is the shape factor characterizing the geometrical effect of the solid particle. For $B \to 0$, the boundary becomes

the z axis with no solid volume; for $B = 1$ the solid becomes a sphere, and for $B \to \infty$ the solid occupies the entire inner cylinder. In the cylindrical geometry, the cylinders are oriented vertically in the direction of heat flux.

In their analysis, Zehner and Schlunder (1970) assume that one-dimensional heat conduction in the unit cell (Fig. 2) follows two parallel paths: the first path is through the fluid in the outer concentric cylinder (of inner radius of unity and outer radius R), and the second path is through the inner cylinder (of unit radius), which is comprised of both the solid and the fluid phases. Thus the effective thermal conductivity of the unit cell is expressed by

$$\frac{k_e}{k_1} = \left(1 - \frac{1}{R^2}\right) + \frac{1}{R^2}\frac{k_{ei}}{k_1} \tag{4b}$$

The quantity k_{ei} is the equivalent thermal conductivity of the inner cylinder, and depends on the shape of the solid-fluid interface A_{fs} given by (Eq. 4a). Based on an analogy with mass transfer experiments, a relation for the unknown R in terms of the porosity is considered as

$$1/R^2 = \sqrt{1-\psi} \tag{4c}$$

For a more detailed derivation of the effective thermal conductivity, the reader is referred to the work of Hsu et al. (1994).

The effective thermal conductivity of a porous packed bed is finally expressed by

$$\frac{k_e}{k_1} = 1 - \sqrt{1-\psi} + \frac{2\sqrt{1-\psi}}{1-\xi B}\left[\frac{(1-\xi)B}{(1-\xi B)^2}\ln\left(\frac{1}{\xi B}\right) - \left(\frac{B+1}{2}\right) - \frac{B-1}{1-\xi B}\right] \tag{5a}$$

where the shape factor B is related to the porosity ψ by the relation

$$\left[\frac{B\left(3 - 4B + B^2 + 2\ln B\right)}{(B-1)^3}\right]^2 = 1 - \psi \tag{5b}$$

and

$$\xi = k_1 / k_2 = 1/\lambda \tag{5c}$$

In the above equations, k_1 and k_2 denote the thermal conductivity of the stagnant fluid and the solid respectively. The porosity ψ appearing in Eqs. (5a) and (5b) is defined by

$$\psi \equiv (\rho_2 - \rho)/(\rho_2 - \rho_1) \tag{5d}$$

where ρ stands for the density of the packed bed (frost in our case), ρ_1 is the density of the fluid (air-vapor in our case), and ρ_2 the density of the solid (ice in our case). It is related to the solids fraction ϕ by the relation

$$\psi = 1 - \phi \tag{5e}$$

It was suggested by Zehner and Schlunder (1970) that Eq. (5b) can be approximated by

$$B = C\left(\frac{1-\psi}{\psi}\right)^m \tag{5f}$$

with $m = 10/9$. The constant C depends on the shape of the particle. Zehner and Schlunder (1970) suggest that $C = 1.25, 1.40$ and 2.5 for spheres, broken (irregular particles) and cylinders respectively.

Cheng and Hsu (1999) point out that the Zehner-Schlunder model (1970) agrees well with the experimental data of Nozad et al. (1985) at $\psi = 0.4$, involving spherical inclusions for $k_2 / k_1 < 10^3$. For $k_2 / k_1 > 10^3$, the Zehner-Schlunder model underpredicts the effective stagnant thermal conductivity substantially. Hsu et al. (1994) postulated that for $k_2 / k_1 > 10^3$ solid-solid conduction through the finite contact area between the spherical particles (arising from flattening of spheres due to external loads or the weight of the bed itself) becomes the main mechanism of heat transfer, and that the reason for this underprediction of data for

$k_2/k_1 > 10^3$ is the assumption of point contacts between spheres. For values of $k_2/k_1 < 10^3$, heat conduction through the finite contact area is of lesser importance, and heat transport is primarily controlled by the particle-fluid-particle conduction. A detailed comparison of Zehner-Schlunder model with data for k_2/k_1 ranging from 8 to 1200 and for various values of solids fraction was recently presented by the author (2010).

5.2. Effect of Mass Diffusion

The effective thermal conductivity of air in the presence of vapor diffusion can be expressed as

$$k_{1d} = k_1 + k_d \tag{6}$$

where k_d is the contribution of mass diffusion to the effective thermal conductivity of air. The contribution of thermal radiation to the effective conductivity of air is neglected relative to the effects of diffusion (Dietenberger 1983).

The mass diffusion contribution k_d is determined from (Sahin 2000)

$$k_d = h_{sv} D \rho_a \frac{d\omega}{dT_f} \tag{7}$$

where ω denotes the local humidity ratio of moist air in the frost layer (assuming equilibrium), h_{sv} the latent heat of sublimation, D the mass diffusivity of water vapor. We can rewrite Eq. (7) in the form

$$k_d = h_{sv} D \rho_a \frac{d\omega}{dp_g} \frac{dp_g}{dT_f} \tag{8}$$

where

$$\omega = 0.622 p_v / p_a \tag{9}$$

$$p_a = p_t - p_v \tag{10}$$

In the above equations, p_t is the ambient (total) pressure (taken as 1 atm here), p_v is the partial pressure of water vapor, and p_a the partial pressure of dry air. The mass diffusivity is determined from (Pruppachar and Eklett, 1978) as

$$D = 2.11\text{x}10^{-5}\left(T_f / T_0\right)^{1.94} \quad \text{m}^2/\text{s} \tag{11}$$

where T_f is the frost temperature in degrees Kelvin, and T_0 the reference temperature (273.15 K). The partial pressure p_v at temperature T_f is given by the Clasius-Clapeyron equation

$$p_v = p_{v0} \exp\left[\frac{h_{sv}}{R_v}\left(\frac{1}{T_0} - \frac{1}{T_f}\right)\right] \tag{12}$$

where p_{v0} stands for the partial pressure of water vapor at reference temperature T_0, and R_v the gas constant for water vapor. Noting that

$$\rho_a \approx p_t / \left(R_a T_f\right) \tag{13}$$

we express Eq. (8) in the form

$$k_d = h_{sv}^2 \frac{D\left(M_a / M_v\right)}{R_v^2 T^3} p_{v0} \exp\left[\frac{h_{sv}}{R_v}\left(\frac{1}{T_0} - \frac{1}{T_f}\right)\right] \tag{14}$$

where M_a, M_f denote the molecular weights of air and water vapor respectively.

5.3. Effect of Eddy Convection

Most of the data on frost thermal conductivity measurements were obtained for flow of moist air under forced convection, while the remainder belong to natural convection. At relatively higher densities the frost becomes a mesh of dendrites with enclosed air pockets

(Biguria and Wenzel 1970). It is therefore plausible that a component of this air flow is directed transverse to the frost layer composed of surface roughness elements, thus randomly penetrating the voids and enhancing the energy transport by turbulent eddy convection.

In the presence of mass diffusion and eddy convection, the effective thermal conductivity of air may be expressed as

$$k_{1dc} = k_1 + k_d + k_c \tag{15}$$

where k_c denotes the contribution of eddy convection to the effective conductivity of air.

By a comparison of their experimental data for frost conductivity and analysis, Biguria and Wenzel (1970) have arrived at a correlation for the turbulent (eddy) conductivity of air as a function of freestream velocity U_∞ as follows:

$$k_c = 0.00568 U_\infty \text{ W/(m.K)} \tag{16}$$

where U_∞ is expressed in m/s. According to the data of various investigators compiled by Yang and Lee (2004), forced convection measurements were obtained for freestream velocities ranging from 1to 12 m/s. The data compiled by O'Neal and Tree (1985) for cylinders, flat plates, annuli, and parallel plates suggest that the freestream velocities ranged from 0.2 to 17 m/s.

Equation (16) indicates that k_c / k_1 =1.2, 2.4 and 3.5 for U_∞ =5, 10 and 15 m/s respectively, considering $k_1 \approx 0.024$ W/(m.K). This consideration represents the significance of eddy convection in enhancing the effective thermal conductivity of frost by increasing the effective stagnant conductivity of air. This observation explains the considerable scatter in many of the correlations proposed for the effective thermal conductivity of frost as a function of frost density alone.

From a more fundamental consideration, the eddy convection in porous media is intimately related to the phenomenon of *thermal dispersion* (see Cheng and Vortmeyer, 1988; Hsu and Cheng, 1990). Thermal dispersion is manifested on account of microscopic fluid velocity and temperature deviations from the corresponding average values, and results in enhanced heat transport. Thus fluid flow in the pore channels of porous media my be regarded as pseudo-turbulence. Many correlations were proposed for transverse and longitudinal thermal dispersion conductivity, and substantial variation prevails between the various correlations (Du et al., 2003). Experiments on forced convection through porous media suggest that the magnitude of transverse thermal dispersion conductivity is often much larger than that of molecular diffusion, and that the axial thermal dispersion conductivity is negligible relative to the bulk convection (Yu and Li 2004). *Measurements also reveal that thermal dispersion increases as the porosity decreases* (Du et al., 2003).

Hsu and Cheng (1990) proposed correlations for the transverse thermal dispersion conductivity for high and low Reynolds number (Re_f) flows in porous media as:

$$\begin{aligned} \frac{k_d}{k_1} &= D_1 \frac{(1-\psi)}{\psi} Pe_f \quad \mathrm{Re}_f >> 10 \\ &= D_2 \frac{(1-\psi)}{\psi^2} Pe_f^2 \quad \mathrm{Re}_f << 10 \end{aligned} \tag{17a}$$

where
$$Pe_f = \mathrm{Re}_f \, \mathrm{Pr}_f \tag{17b}$$

and
$$\mathrm{Re}_f = u_m d_p / \alpha_f, \quad \mathrm{Pr}_f = \nu_f / \alpha_f \tag{17c}$$

with the subscript denoting the fluid phase. The quantities Pr_f, Pe_f denote respectively the Prandtl number and Peclet number of the fluid, u_m the mean axial velocity of the fluid, and d_p the particle diameter. The constants D_1, D_2 are evaluated by comparison of the model

with measurements. The effect of tortuous flow paths on the constant D_1 for high Reynolds number flow was reported by Yu and Li (2004) with the aid of a fractal model. Transverse thermal dispersion and wall channeling effects (existence of peak velocity in a region close to the external boundary) were treated by Cheng and Vortmeyer (1988). Convection in variable porosity media, including channeling effects, were considered by Vafai (1984).

In the present context of frost growth, the external flow is on the top of the frost layer instead of streaming through the interior of the frost layer in the axial direction transverse to the frost thickness, and only a portion of this external flow is directed into the interior of the frost layer in longitudinal and transverse directions, leading to low Reynolds number flow regime. Thus existing information on the thermal dispersion effects in the traditional packed beds cannot be directly applied to the circumstances of frost formation. Much work remains to be undertaken before quantitative effects of thermal dispersion in frost layers can be addressed with regard to the effective thermal conductivity of frost. A detailed account of thermal dispersion effects in frost layers is beyond the scope of the present work.

5.4. Thermophysical Properties

In the present analysis, the properties are taken as follows. The thermal conductivity of air is calculated as (Rohsenow and Hartnett' 1973; Dietenberger, 1983)

$$k_1 = k_{\text{air}} = 2.646\text{x}10^{-13}\left[\frac{T^{1/2}}{1+(245/T)10^{12/T}}\right]\frac{\text{W}}{\text{m.K}} \tag{18}$$

where T is in degrees Kelvin. The thermal conductivity of ice is obtained from the relation (Dillard and Timmerhaus, 1969; also Dietenberger, 1983)

$$k_2 = k_{\text{ice}} = 630/T \ \text{W/(m.K)} \tag{19}$$

where T is the absolute temperature (degrees K).

The latent heat of sublimation of ice is determined from (Mago et al., 2004)

$$h_{fv} = \{-0.1083[1.8(T-273.16)+32]+2833\} \text{ kJ/kg} \quad (20)$$

where T is in degrees Kelvin.

6. Results and Comparison

6.1 Comparison with Correlations

In the evolving frost layer, the actual structure of the ice particles is very complex, and far from being that of spheres. In an effort to understand the sensitivity of the effective conductivity of porous media on particle shape, calculations with Eq. (5) have been made for spheres, cylinders and irregular particles with $k_2 / k_1 = 100$ in the absence of mass diffusion and eddy convection, and the predicted effective thermal conductivity is compared with the correlations of frost thermal conductivity to density due to Yonko and Sepsy (1967) and of Van Dusen (1929). The results suggest that cylinders lead to the highest effective conductivity with the irregular particles producing slightly higher values than the spheres, and that the cylinder results are closer to the experimental data (correlations) of frost relative to those of spheres and irregular-shaped particles. In view of these considerations, we hypothesize here that the frost particles are better represented by cylinders, and thus we consider only cylinders in our subsequent results.

In the case of cylindrical geometry referred to in the Zehner-Schlunder model, the cylinders are oriented vertically (normal to the plate surface) in the direction of heat flow. This choice of cylinders points to a very real effect in the formation of frost, which can develop anisotropically, with a preferred direction of growth. This consideration might explain why the cylindrical geometry is better suited over spheres in describing the frost thermal conductivity.

The role of mass diffusion on the frost thermal conductivity is illustrated in Fig. 3, with the aid of Eqs. (5), (6), and (14), with k_1 in Eq. (5a) *replaced* by k_{1d}. The mass diffusion effect is shown for three different frost temperatures of 250 K, 260 K, and 273 K (the latter representing the maximum possible value). The conductivity contribution due to mass diffusion increases with an increase in temperature. There is seen a crossover of the curves at large value of ϕ. At $T_f = 273\,\mathrm{K}$, the mass diffusion contribution improves the agreement with data; but even with mass diffusion, there still exists considerable underprediction of the data. Thus additional mechanisms for enhancing the frost conductivity seem to exist.

Figure 4 presents the predictions of k_{ef} with mass diffusion and eddy convection on the basis of Eqs. (5) and (14-15), with k_1 in Eq. (5a) *replaced* by k_{1dc}. The diffusion contribution is taken at $T_f = 273\,\mathrm{K}$, and an eddy convection factor $k_c / k_1 = 1$ is considered. The increase in the conductivity due to eddy convection is of the same order as that due to mass diffusion. In the Yonko and Sepsy 's data, the air velocities range of 1.3 to 5.3 m/s roughly correspond to k_c / k_1 of about 0.3 to 1.25 (an average of about 0.8) in accordance with Eq. (16). With the inclusion of eddy convection effect, the agreement between the theory and the data has improved. In particular, the theory accounting for combined diffusion and convection matches closely with Van Dusen's correlation up to about $\phi = 0.4$, but still significantly underpredicts the conductivity expressed by the Yonko-Sepsi correlation. A frost temperature of 273 K is slightly unrealistic in terms of experimental considerations, and so are the conditions of natural convection in the experiments.

The effect of eddy convection levels on the effective thermal conductivity of frost, as computed from Eqs. (5) and (14-15), is demonstrated in Fig. 5. The comparisons are shown

for k_c / k_l =1, 2 and 3, and at T = 273 K. It is observed that with increasing value of the eddy convection, the effective frost conductivity increases, as is to be expected. Recall that the Yonko-Sepsy correlation constitute data for which k_c / k_l ranges from 0.3 to 1.25. For $\phi < 0.6$, better agreement is achieved between the prediction and the Yonko-Sepsy correlation with a choice of $k_c / k_l = 3$. In the case of Van Dusen correlation, the condition of k_c / k_l =1 affords better accord between the theory and the correlation up to $\phi = 0.4$. It appears that a mean value of $k_c / k_l = 2$ may be regarded as reasonable considering the full range of frost density. It appears that the value of $k_c / k_l = 3$ represent the high end of free stream velocity values, and are not as realistic as k_c / k_l =1 or 2.

A comparison of the present theory, according to Eqs. (5) and (14-15), with the correlation of Sturm et al. (1997) is depicted in Fig. 6. The data are obtained for mean temperature of about 258 K cover various types of snow, having different microstructure, and as a result show considerable scatter. The results from Van Deusen (1929) correlation and from Östin and Anderson (1991) correlation are also shown for comparison purposes. For solid fractions ϕ between 0.2 and 0.5, the theory is closer to Van Deusen and Östin and Anderson correlations, whereas for $\phi > 0.5$ the theory agrees better with the correlation of Sturm et al. (1997) and of Östin and Anderson correlation, which extends up to the farthest value of $\phi \approx 0.74$.

6.2 Comparison with Measurements

Figure 7a illustrates a comparison of the present theory, given by Eqs. (5) and (14-15), with the data for the frost conductivity obtained by Pitman and Zuckerman (1967) and Kaempfer et al. (2005). Eq. (18) is used to obtain the thermal conductivity of air. Both the

measurements correspond to an average temperature of 246 K. With regard to the data of Pitman and Zuckerman (1967), the snow used in the experiments was composed of vapor grown crystals having length of 3 to 5 mm. The estimated uncertainty in the measured conductivity is about 10 percent. In the measurements of Kaempfer et al. (2005) the snow sample is 2 cm high and 4.8 cm in diameter, with the data taken at a single density of 268 kg/m^3. The measured conductivity is 0.18 ± 0.02 M/m.K. The snow microstructure was imaged by X-ray micro-tomography. The predicted snow conductivity from their microstructural numerical model (based on some assumed structural parameters, and accounting for conduction mechanism only) was found to be 0.15 ± 0.01 W/m.K.

The comparisons suggest that the present theory, accounting for mass diffusion and an eddy convection factor $k_c / k_1 = 1$, matches the data satisfactorily over a broad range of solid fraction up $\phi = 0.45$ (density of 450 kg/m^3). Only at $\phi = 0.54$ the theory with $k_c / k_1 = 2$ offers a better agreement with the data. The relatively close agreement between the two sets of data at $\phi = 0.29$ (density of 268 kg/m^3) should serve as a testament to the reliability of the data over the particular range of frost density. These comparisons suggest the importance of mass diffusion and eddy convection phenomena in governing the effective thermal conductivity of frost.

Figure 7b shows a comparison of the predicted frost conductivity, provided by Eqs. (5) and (14-15), with the data of Pitman and Zuckerman (1967) for temperatures of 185 K, 246 K and 268 K. These data are the most widely cited data, and were obtained with an artificial snow (freezer frost) with a steady state measuring method. Note that in the ordinate the dependence of air thermal conductivity with temperature $k_1(T)$ is taken into account. The results suggest that the data for thermal conductivity at different temperatures (covering a

wide temperature range) when presented in dimensionless form nearly collapse up to ϕ of about 0.45, and in this range excellent agreement between the theory and the data is noticed. For $\phi > 0.5$, the measured conductivity at the highest temperature of 268 K considerably exceeds the predictions. According to Sturm et al. (1997), the reliability of the measurements of Pitman and Zuckerman (1967) is questionable.

The comparisons presented in Figs. 7a and 7b, suggesting that the model underpredicts the data for the effective frost thermal conductivity for ϕ exceeding about 0.5, reveal that thermal dispersion effect likely increases with solids fraction in this region. This is qualitatively consistent with the measurements on packed beds suggesting that thermal dispersion effect increases as the porosity decreases (Du et al., 2003).

A comparison of the model predictions from Eqs. (5) and (14-15) with the experimental data of Brian et al. (1970) for the average thermal conductivity at $T_f = 175\,\mathrm{K}$ is shown in Fig. 8. Thermal conductivity of air is obtained from Eq. (18). The data are limited to relatively low density frost having density ranging from 50 to130 kg/m^3 , The conductivity data are obtained from transient measurements. The average thermal conductivity of the frost layer was determined from the measured values of the heat flux, the average temperature difference across the frost, and the frost thickness (Fourier's law). The scatter in the data is believed to be due to structural differences in the frosts of the same density, and due to differences in the freestream velocity and humidity. The present theory based on mass diffusion and an eddy convection factor of one agrees favorably with the measurements. These comparisons, although restricted to a relatively lower range of frost density, appear to be consistent with those presented in Fig. 7, and serve to support the validity and usefulness of the proposed model.

7. Discussion

The present results suggest that cylindrical inclusions may better represent the frost inner structure. As the heat transfer in frost is anisotropic, the model presented here is not expected to be applicable to the prediction of the effective thermal conductivity of frost in the direction perpendicular to the main axes of the cylindrical inclusions. However in most of the one-dimensional formulations of heat and mass transfer during frost growth, it is the effective thermal conductivity of frost in the direction of heat flow that is required. A detailed account of two-dimensional thermal conduction in frost layers is beyond the scope of the present investigation.

8. Conclusions

The Zehner-Schlunder model for the effective thermal conductivity of porous media has been extended to describe the effective thermal conductivity of frost. By superposing the physical effects of mass diffusion and eddy convection on the molecular thermal conductivity of air, as expressed by Eqs. (14) and (15), the proposed model yields estimates for the effective thermal conductivity of frost, given by Eq. (5), as a function of frost density and temperature over the full range of frost density. Comparisons of the model predictions with the well-known correlations and measurements for frost conductivity suggest that the frost may be better represented by an assemblage of cylinders rather than spheres. The proposed model reveals that both mass diffusion and eddy convection effects have significant effect on the frost thermal conductivity, and are of the same order.

Acknowledgments

The author is grateful to the reviewers for their valuable suggestions and criticism in improving the manuscript.

References

Abels, H., Rep. Meteor., Vol. 16, No. 1, 1893.

Andrews, T., Observations on pure ice and snow, Proc. R. Soc., London, Vol. 40, pp. 544-549, 1886.

Arons, E.M. and Colbeck, S.C., Geometry of heat and mass transfer in dry snow: a review of theory and measurement, Reviews of Geophysics, Vol. 33, pp. 463-493, 1995.

Arons, E.M., and Colbeck, S.C., Effective medium approximation for the conductivity of sensible heat in dry snow, In. J. Heat Mass Transfer, Vol. 41, pp. 2653-2666, 1998.

Auracher, H., Effective thermal conductivity of frost, in: Proceedings of the International Symposium of Heat and Mass Transfer in Refrigeration Cryogenics, Dubrovnik, pp. 285-302, 1986.

Biguria, G. and Wenzel, L.A., Measurement and correlation of water frost conductivity and density, I&EC Fundamentals 9 (1970) 129-138.

Brian, P.L.T., Reid, R.C., Y.T. Shah, Y.T., Frost deposition on cold surfaces, I&EC Fundamentals, Vol. 9, pp. 375-380, 1970.

Burghardt, M.D., Engineering Thermodynamics with Applications, second ed., Harper & Row Publishers, New York, 1972.

Cheng, P. and Hsu, C-T., The effective stagnant thermal conductivity of porous media with periodic structures, J. of Porous Media, Vol. 2, pp. 19-38, 1999.

Cheng, P. and Vortmeyer, D., Transverse thermal dispersion and wall channeling in a packed bed with forced convective flow, Chem. Engng. Sci., Vol. 9, pp. 2523-2532, 1988.

Cheng, C-H and Wu, K-K, Observations of early-stage frost formation on a cold plate in atmospheric air flow, ASME J. of Heat Transfer, Vol. 125., pp. 95-102, 2003.

Coles, W.D., Experimental determination of thermal conductivity of low density ice, NACA Technical Note 3143, 1954.

Deveaux, J., Radiothermic economy of fields of snow and glaciers, Science Abstracts Series A, Vol. 36, pp. 980-981, 1933; abstracted from Ann. d. Physics, Vol. 20, pp. 5-67, 1933.

Dietenbeger, M.A., Generalized correlation of the water frost thermal conductivity, Int. J. of Heat Mass Transfer, Vol. 26. pp. 607-619, 1983.

Dillard, D.S., and Timmerhaus, K.D., Low temperature thermal conductivity of selected dielectric crystalline solids, in Thermal Conductivity, in: by C.T. Ho and R.E. Taylor (Ed.), Proceedings of the 8th Conference, Plenum Press, New York, 1969, pp. 949-967.

Du, J., Hu, X., and Wang, B-X, Thermal dispersion model for single phase flow in porous media, Heat transfer- Asian Research, Vol. 32, pp. 545-552, 2003.

Emery, E.F., and Siegel, B.L., Experimental measurements of the effects of frost formation on heat exchanger performance, Proceedings of AIAA/ASME Thermophysics and Heat Transfer Conference, Heat and Mass Transfer in Frost and Ice Packed Beds and Environmental Discharges, in: R.B.V. Armili, D.E., S. Sengupta, S. (Eds.), ASME HTD-139, pp. 1-7, 1990.

Feng, Y., Yu, B., Zou, M., and Xu, P., A generalized model for t he effective thermal conductivity of unsaturated media based on self-similarity, J. Porous Media, Vol. 10, pp. 551-568, 2007.

Hayashi, Y., Aoki, A., Adachi, S., and Hori, K., Study of frost properties correlating with frost formation types, ASME J. of Heat Transfer, Vol. 99, pp. 239-245, 1977.

Hertz, H., J. Math. (Crelle's Journal), Vol. 92, 1988.

Hsu, C.T., Cheng, P., and Wong, K.W., Modified Zehner-Schlunder models for stagnant thermal conductivity of porous media, Int. J. of Heat Mass Transfer, Vol. 37, pp. 2751-2759, 1994 .

Hsu, C. T. and Cheng, P., Thermal dispersion in a porous medium, Int. J. of Heat and Mass Transfer, Vol. 33, pp. 1587-1597, 1990.

Jansson, J., Ofvers. af K.. Svenska Vet. Akad. , Vol. 58, pp. 207-222, 1901.

Le Gall, R., Grillot, J.M., and Jallut, C., Modeling of frost growth and densification, Int. J. of Heat Mass Transfer, Vol. 40, pp. 3177-3187, 1997.

Kamei, S., Mizushina, T., Kifune, S., and Koto, T., Research on frost formation in a low temperature dehumidifier, Chem. Eng. of Japan, Vol. 14, p. 53, 1950.

Kaempfer, T.U., Schneebeli, M., and Sokratov, S.A., A microstructural approach to model heat transfer in snow, Geophys. Res. Lett., Vol.32, L21503, 2005.

Kandula, M., On the effective thermal conductivity of porous packed beds with uniform spherical particles, ***accepted for publication*** *in* J. of Porous Media, February 2010.

Kaviany, M., Principles of Heat Transfer in Porous Media, Springer-Verlag, New York, 1995.

Kondrateva, A.S., Thermal conductivity of snow cover and physical process caused by the temperature gradient, S.I.P.R.E. Translation No. 22, 1954.

Mago, P.G. and Sheriff, S.A., Frost formation and heat transfer on a cold surface in ice fog, AIAA-2004-164, 2004.

Maxwell, J.C., A Treatise on Electricity and Magnetism, Clarendon Press, Oxford, 1873, p. 365.

Nozad, S., Carbonell, R.G., and Whitaker, S., Heat conduction in multiphase systems, I: Theory and experiments for two-phase systems, Chem. Eng. Sci., Vol. 40., pp. 843-855, 1985.

O'Neal, D.L. and Tree, D.R., A review of frost formation in simple geometries, ASHRAE Trans., Vol. 91. pp. 267-281, 1985.

Östin, R. and Anderson, S., Frost growth parameters in a forced air stream, Int. J. of Heat Mass Transfer, Vol. 34 (4/5), pp. 1009-1017, 1991.

Pitman, D., and Zuckerman, B., Effective thermal conductivity of snow at -88^0, -27^0, and -5^0C, J. of Applied Phys., Vol. 38, pp. 2698-2699, 1967.

Pruppacher, H.R. and Klett, J.D., Microphysics of Clouds and Precipitation, Reidel, Dordrecht, 1978.

Rayleigh, Lord, On the influence of obstacles in rectangular order upon the properties of a medium, Phil. Mag., Vol. 34, pp. 481-502, 1892.

Rosenow, W.M. and Hartnett, J.P., Handbook of Heat Transfer, McGraw-Hill, New York, 1973.

Sahin, A.G., Effective Thermal conductivity of frost during the crystal growth period, Int. J. of Heat Mass Transfer, Vol. 43, 539-553, 2000.

Sami, S.M. and Duong, T., Mass and heat transfer during frost growth, ASRAE Transactions, Vol. **95**, pp. 158-165, 1989.

Schropp, K., Investigation of dew and frost formation on cooling tubes in still air and the influence upon the heat transfer, Zeitschr. ges. katte. Ind., Vol. 42, pp. 81-85, 127-131, 151-154, 1935

Shin, J., Tikhonov, A.V., and Kim, C., Experimental study on frost structure on surfaces with different hydrophilicity: density and thermal conductivity, ASME J. of Heat Transfer, Vol. 125, pp. 84-94, 2003.

Sturm, M., Holmgen, J., Konig, M., and Morris, K., The thermal conductivity of seasonal snow, J. Glaciology, Vol. 43, pp. 26-41, 1997.

Tien, C.L. and Vafai, K., Statistical bounds for the effective thermal conductivity of microsphere and fibrous insulation, AIAA Progress Series, Vol. 65, pp. 135-148, 1979.

Timoshenko, S.P. and Goodier, J.N., Theory of Elasticity, third ed., McGraw-Hill Book Co., New York, 1970.

Vafai, K., Convective flow and heat transfer in variable-porosity media, J. Fluid Mechanics, Vol. 147, pp. 233-259, 1984.

Van Dusen, M.S., *International Critical Tables* 5, McGraw-Hill Book Co., p. 216, 1929

Woodside, W., Calculation of the thermal conductivity of porous media, Canadian J. of Phys., Vol. 36, pp. 815-823, 1958.

Yang, D-K and Lee, K-S, Dimensionless correlations of frost properties on a cold plate, Int. J. of Refrigeration, Vol. 27, pp. 89-96, 2004.

Yonko, J.D. and Sepsy, C.F., An investigation of the thermal conductivity of frost while forming on a flat horizontal plate, Paper No. 2043, Presented at ASHRAE 74th Annual Meeting, Minnaepolis, MN, 1967.

Yu, B. and Cheng, P., Fractal models for the effective thermal conductivity of bidispersed porous media, J. Thermophysics and Heat Transfer, Vol. 16, pp. 22-29, 2002.

Zehner, P. and Schlunder, E.U., Thermal conductivity of granular materials at moderate temperatures (in German), Chemie Ingr. Tech., Vol. 42, pp. 933-941, 1970.

Figure Captions

Figure 1(a). Representation of frost structure during various stages of frost growth.

Figure 1(b). Representation of ice crystal structure (Sahin, 2000).

Figure 1(c). Representation of heat and mass transport by diffusion and convection in a frost layer.

Figure 2. Schematic of the unit cell in Zehner-Schlunder model (1970).

Figure 3. Effect of mass diffusion on the effective thermal conductivity of frost at various frost temperatures.

Figure 4. Effect of mass diffusion and eddy convection on the effective thermal conductivity of frost at 273 K.

Figure 5. Dependence of thermal conductivity of frost on mass diffusion and eddy convection for various eddy convection coefficients.

Figure 6. Comparisons of predicted thermal conductivity of frost with the correlations of Sturm et al. (1997), Van Deusen (1929), and Östin and Anderson (1991).

Figure 7a. Comparisons of predicted thermal conductivity of frost with the measurements of Pitman and Zuckerman (1967) and Kaempfer et al. (2005) at 246 K.

Figure 7b. Comparisons of predicted thermal conductivity of frost with the measurements of Pitman and Zuckerman (1967) and Kaempfer et al. (2005) at various temperatures.

Figure 8. Comparisons of predicted thermal conductivity of frost with the measurements of Brian et al (1970).

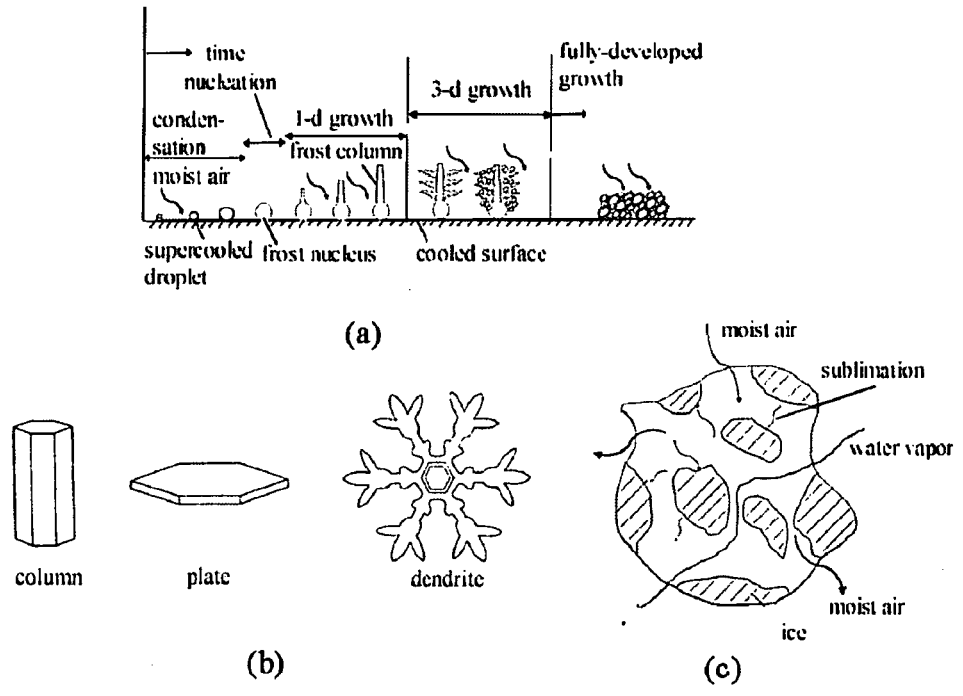

Figure 1. (a) Representation of frost structure during various stages of frost growth, (b) Representation of ice crystal structure (Sahin 2000), (c) Representation of heat and mass transport by diffusion and convection in a frost layer.

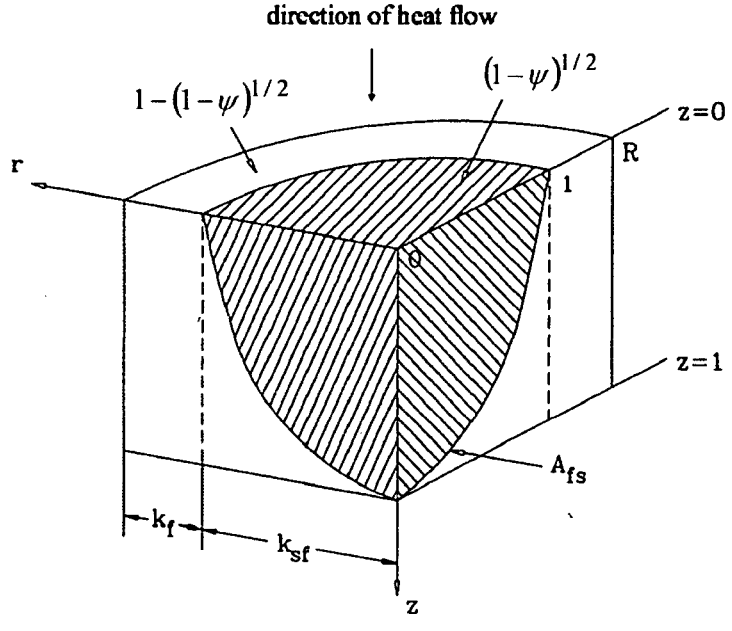

Figure 2. Schematic of the unit cell in Zehner-Schlunder model (1970).

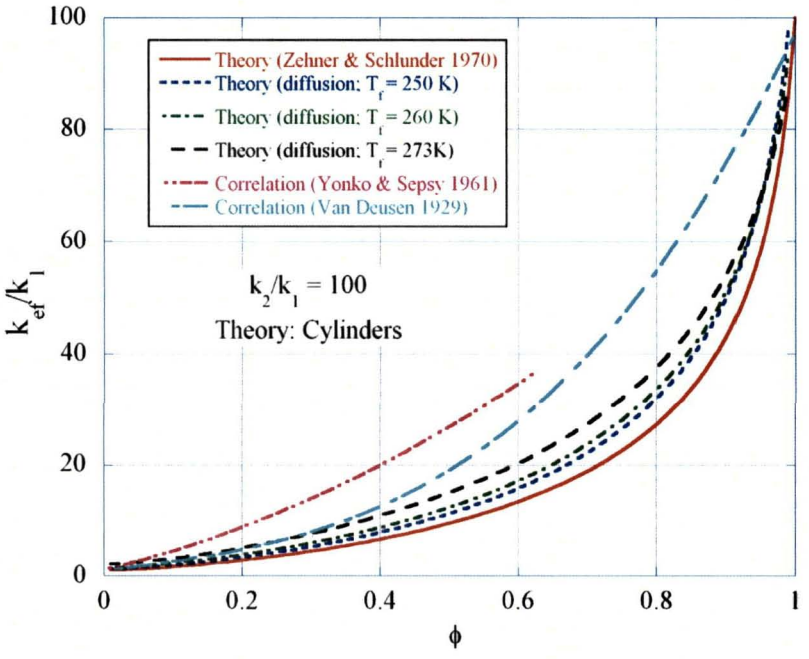

Figure 3. Effect of mass diffusion on the effective thermal conductivity of frost at various temperatures.

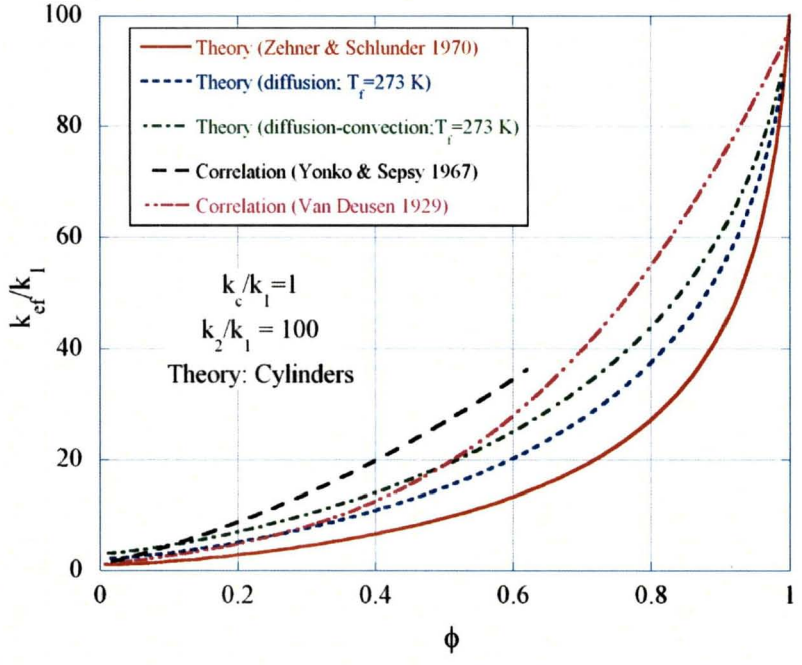

Figure 4. Effect of mass diffusion and eddy convection on the effective thermal conductivity of frost at 273 K.

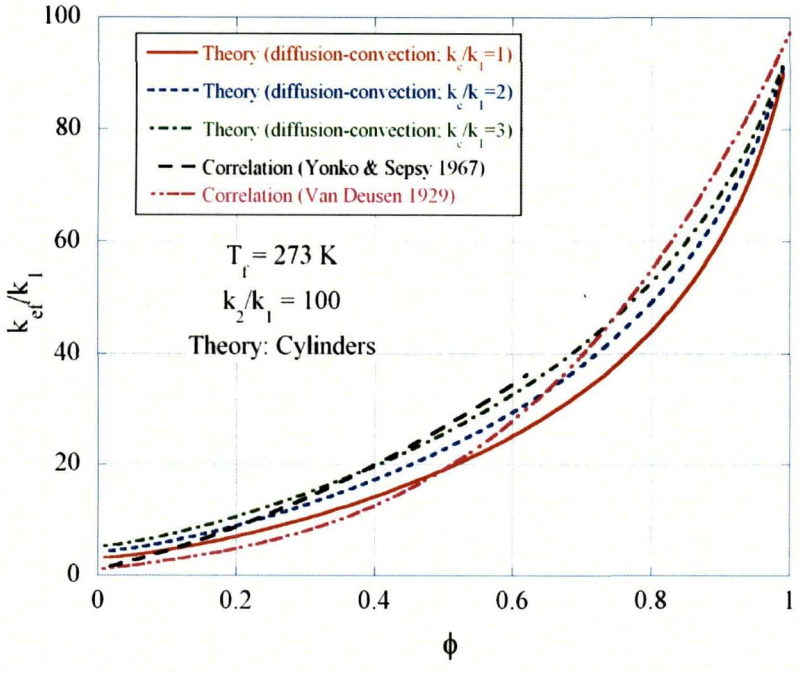

Figure 5. Dependence of thermal conductivity of frost on mass diffusion and eddy convection for various eddy convection coefficients.

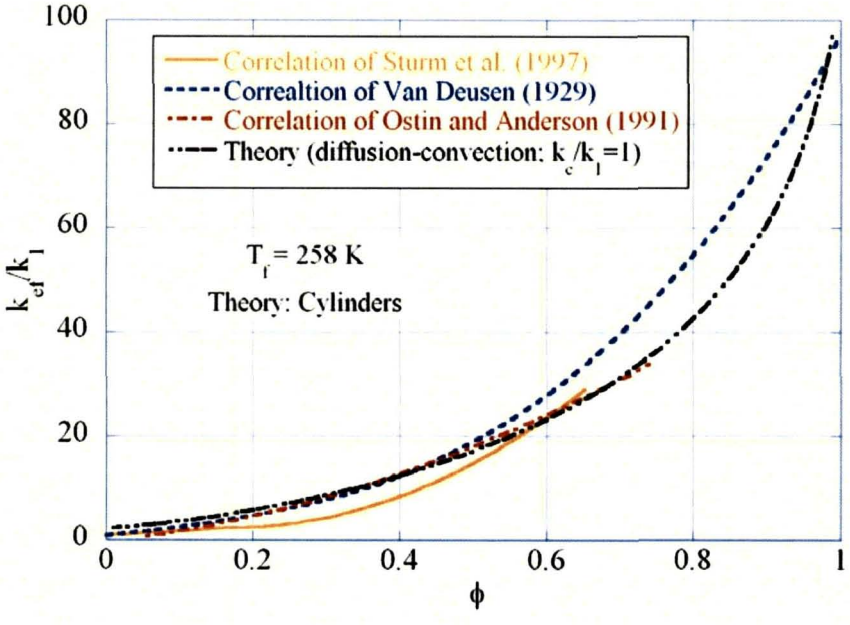

Figure 6. Comparisons of predicted thermal conductivity of frost with the correlations of Sturm et al. (1997), Van Deusen (1929), and Ostin and Anderson (1991).

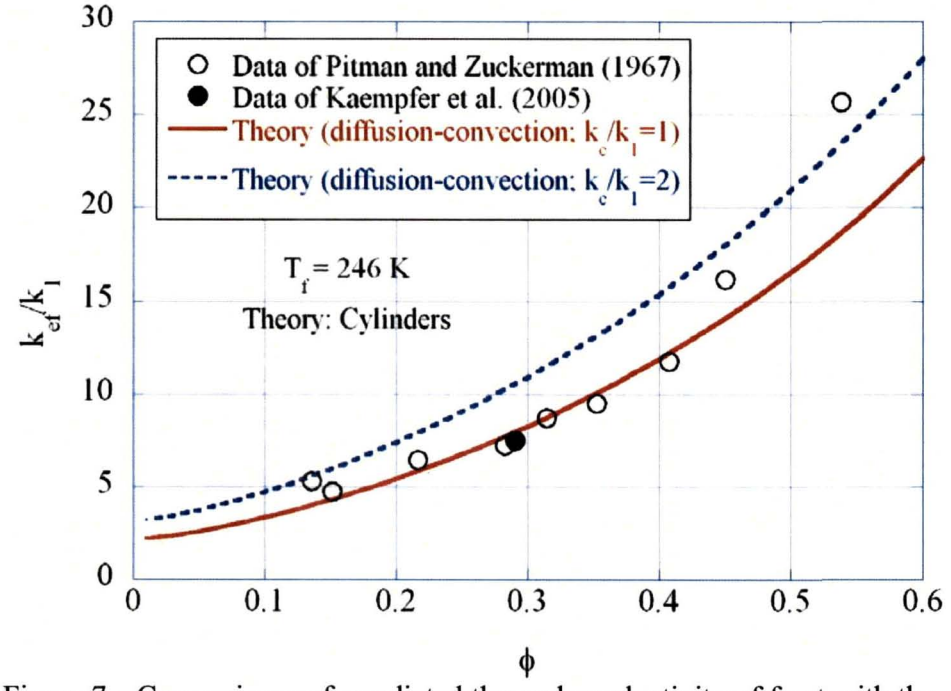

Figure 7a. Comparisons of predicted thermal conductivity of frost with the measurements of Pitman and Zuckerman (1967) and Kaempfer et al. (2005) at 246 K

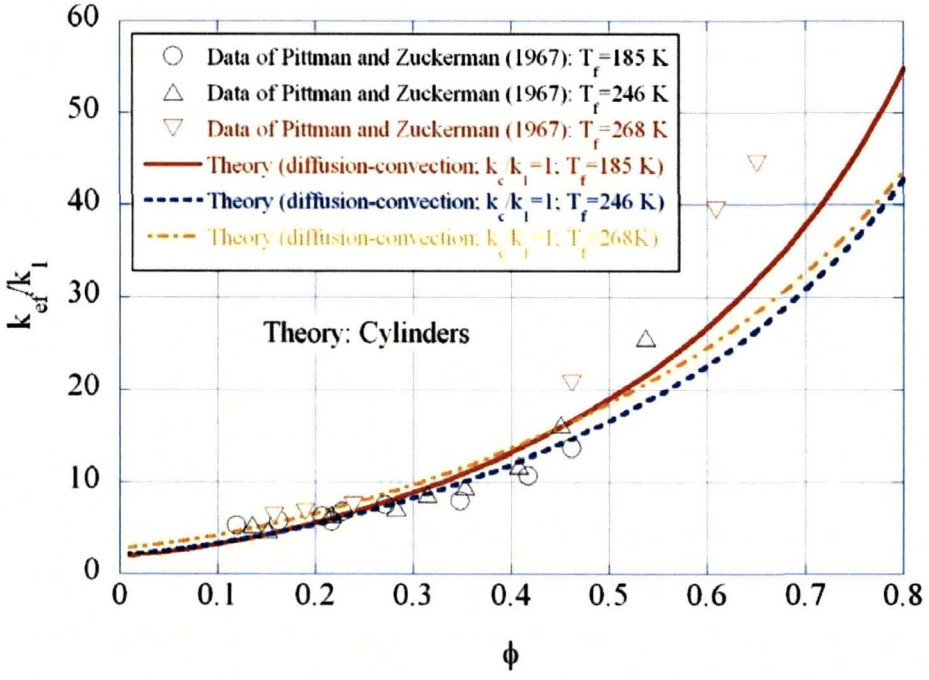

Figure 7b. Comparisons of predicted thermal conductivity of frost with the measurements of Pitman and Zuckerman (1967) and Kaempfer et al. (2005) at various temperatures.

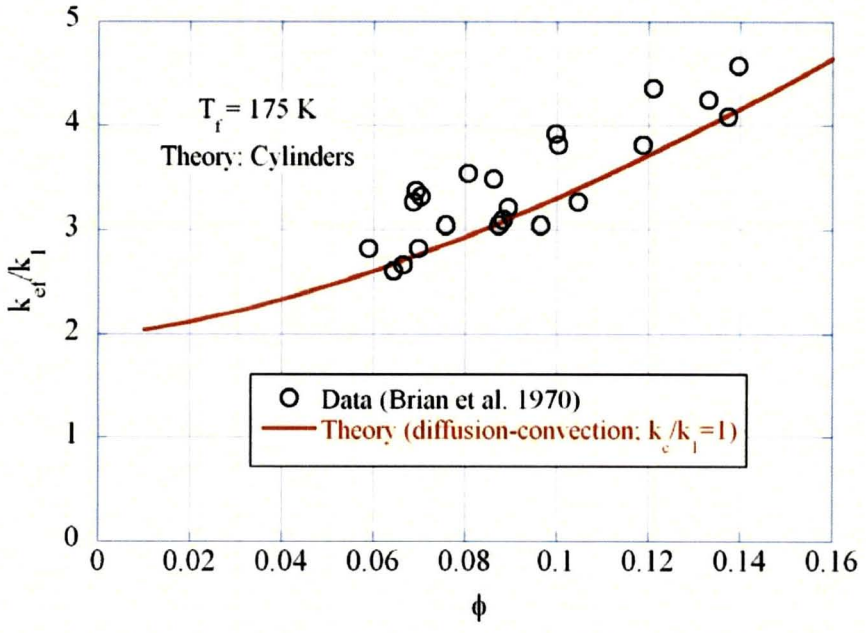

Figure 8. Comparisons of predicted thermal conductivity of frost with the measurements of Brian et al (1970) at various temperatures.